Site−Site Potentials in Neopentane and Tetramethylsilane

Michael W. P. Petryk and Bryan R. Henry*

Department of Chemistry, University of Guelph, Guelph, Ontario N1G 2W1, Canada

Martin L. Sage

Chemistry Department, Syracuse University, Syracuse, New York 13244

Received: June 14, 2005; In Final Form: September 6, 2005

Neopentane and TMS are used as model $M(CH_3)_4$ systems to investigate *intramolecular* interactions. The nonbonded site−site potential between two proximal hydrogen atoms on different methyl groups, $V_{nb}(d_{HH})$, is not Lennard−Jones- or Morse-like but is found to be pseudolinear in hydrogen−hydrogen internuclear separation, d_{HH}, for both neopentane and TMS. The Morse potential is found to be a poor basis in which to expand $V_{nb}(d_{HH})$. The nonbonded site−site potential is conformation-dependent and not transferable between molecules. The individual contributions to $V_{nb}(d_{HH})$ are presented. The local mode parameters for neopentane and TMS are calculated ab initio for a variety of molecular conformations. The ab initio values of the local mode frequency and local mode anharmonicity are increasingly blue-shifted with increasing steric hindrance. Electron correlation is found to be increasingly important with decreasing internuclear separations, d_{HH}.

Introduction

In a previous paper,[1] we found that collision-like through-space interactions perturb low-energy (fundamental)[1] and high-energy[1,2] vibrational spectra, as well as promote mixing between torsional and vibrational states.[1,3,4] Such interactions can lead to unexpectedly broad vibrational overtone spectra.[1] This paper deals with the nature of through-space interactions and their functional form.

We are specifically interested in the difference between nonbonded intramolecular interactions (e.g., through-space coupling) and nonbonded intermolecular interactions. We identify both of these nonbonded interactions as site−site interactions in the sense that we can approximate a nonbonded interaction by a potential between two sites. In the case of through-space coupling, these two sites are two atoms within a molecule.

Previous work[5,6] suggests that at very short internuclear separations, conventional site−site treatments are lacking. For example, the simple 9-6 Lennard−Jones-type model for van der Waals interactions may not be suitable for sterically hindered molecules such as *cis*-2-butene where there is a short nonbonded distance between proximal methyl hydrogens.[5] Force fields often cannot predict vibrational frequencies in "overcrowded" molecules because they do not properly account for nonbonded potentials when atoms are in very close proximity to one another.[6]

Hydrogen atoms are very common in molecular systems, especially biological ones. We will restrict our investigation of site−site potentials to hydrogen−hydrogen interactions. For systems containing many hydrogen atoms, these interactions will be expressed in terms of hydrogen−hydrogen separation between proximal H atoms, d_{HH}.

* Corresponding author. E-mail: chmhenry@uoguelph.ca.

Theory and Calculations

Local Modes and the Morse Potential. Within the local mode model, the *X*H stretching potential is often described as a Morse potential[7,8]

$$V(q) = D_e(1 - e^{-aq})^2 \tag{1}$$

where q is the displacement from equilibrium of the *X*H bond, D_e is the depth of the potential well, and a is the characteristic Morse inverse length that can be obtained from the Morse frequency, $\tilde{\omega}$, and anharmonicity, $\tilde{\omega}x$.[8] A more generalized Morse potential[9] is obtained by expanding eq 1 in terms of q to obtain

$$V(q) = D_e(1 - e^{-b_1q+b_2q^2+b_3q^3+b_4q^4+b_5q^5})^2 \tag{2}$$

where b_i are expansion coefficients. The energy eigenvalues of a Morse oscillator described by eq 1 can be rearranged to give the frequency, $\tilde{\nu}_{v\leftarrow 0}$, of an overtone transition out of the ground state $v' = v \leftarrow v'' = 0$[8]

$$\tilde{\nu}_{v\leftarrow 0} = v\tilde{\omega} - (v^2 + v)\tilde{\omega}x \tag{3}$$

The values of the Morse parameters $\tilde{\omega}$ and $\tilde{\omega}x$ are obtained from a quadratic fit of $\tilde{\nu}_{v\leftarrow 0}$ versus v.

Isolated Anharmonic (Morse) Oscillator. For *X*H stretching vibrational overtone transitions, the coupling between *X*H oscillators in which the H atoms do not share a common atom (e.g., benzene, etc.) is negligible.[10−13] The *X*H stretching Hamiltonian for a molecule composed of i isolated *X*H oscillators becomes

$$\hat{H} = \frac{1}{2}\sum_i G_{ii}p_i^2 + \sum_i D_{e_i}(1 - e^{-a_iq_i})^2 \tag{4}$$

10.1021/jp058187+ CCC: $30.25
Published on Web 10/13/2005

where the first term is the sum of the (diagonal) kinetic energy and the second term is the sum of the (diagonal) anharmonic potential energy. The frequencies of transitions out of the ground vibrational state for any single oscillator, *i*, is given by 3.

Force Constants and Their Relationship to Morse Oscillator Parameters. The stretching potential of an isolated *X*H oscillator can be expressed as[14]

$$V(q) = \frac{1}{2} f_{ii} q^2 + \frac{1}{6} f_{iii} q^3 + \frac{1}{24} f_{iiii} q^4 \quad (5)$$

where the *f* terms represent diagonal *X*H force constants. If the potential given by eq 5 is equated with the Morse potential (eq 1), then the following correspondences can be drawn between the Morse parameters and the diagonal force constants[14]

$$\tilde{\omega} = \frac{\sqrt{g_{ii} f_{ii}}}{2\pi c} \quad (6)$$

and

$$\tilde{\omega}x = \frac{h g_{ii}}{72\pi^2 c} \left(\frac{f_{iii}}{f_{ii}}\right)^2 \quad (7)$$

where g_{ii} is the Wilson G-matrix element.

Fitting Ab Initio Data to Morse Potentials. Ab initio data have been fit to Morse potentials in three different ways, namely, (1) a power series fit to eq 5 where $\tilde{\omega}$ and $\tilde{\omega}x$ are obtained from the diagonal *X*H force constants, (2) a nonlinear fit to eq 1 where $\tilde{\omega}$ and $\tilde{\omega}x$ are obtained from parameters D_e and *a*, and (3) a nonlinear fit to eq 2 where the expansion coefficients, b_i, are obtained. In all three methods, the fit was carried out using nine data points from ab initio calculations in which the CH bond displacement was varied in steps of 0.05 Å (vide infra) to ensure the convergence of the expansion terms.[15,16] The relative benefits of these approaches are detailed below.

A power series fit to eq 5 is computationally inexpensive and straightforward. This approach has therefore been favored historically. A drawback of this approach is that the local mode parameters are approximated by a truncated power series, introducing uncertainties into $\tilde{\omega}$ and $\tilde{\omega}x$.

A nonlinear fit to eq 1 furnishes $\tilde{\omega}$ and $\tilde{\omega}x$ in a straightforward manner. The benefit of this approach is that the local mode parameters are arrived at without having to resort to approximation by a truncated power series. A drawback of this approach is that nonlinear fits are more computationally intensive and can be more unstable than a power series fit. Nonlinear fits have thus not been used as much as power series fits in past investigations.

A nonlinear fit to eq 2 is used to determine the suitability of the Morse potential as a basis in which to expand the ab initio calculated *X*H stretching potential. The expansion terms, b_i, resulting from this fit to ab initio data cannot be related to the local mode parameters, $\tilde{\omega}$ and $\tilde{\omega}x$, in a straightforward manner. Instead, the standard deviation in the fit of the ab initio stretching potential to eq 2 is used to quantify the deviation from Morse-like behavior and provides a sensitive tool for investigating the effect of molecular conformation on the "Morseness" of the *X*H stretching potential.

Scaling Ab Initio Calculated Frequencies and Anharmonicities. Local mode scaling factors, either individual or averaged over a large number of molecules,[15] are highly dependent on the manner in which they are calculated. Specifically, local mode scaling factors are dependent upon (1) theory and basis set, (2) displacement grid (i.e., the displacement range, and to a lesser degree upon the step size), (3) the fit type used to extract the local mode parameters (e.g., a power series fit to eq 5 or a nonlinear fit to eq 1), and (4) the degree of steric hindrance of the *X*H oscillator being modeled.

In the interest of accuracy, scaling factors specific to individual molecules (at a given theory level and basis set) have been developed previously[17] and will be used in this paper. These scaling factors were calculated from ab initio data obtained in the range $q = [-0.20, 0.20]$ Å in steps of 0.05 Å at HF/6-311++G(2d,2p) and fit to a power series (eq 5) or a nonlinear fit (eq 1).

Computational Details

Ab initio calculations were carried out with Gaussian 98 revision A.5[18] on a SGI Octane with a MIPS R10000 processor, Gaussian 98 revision A.11[19] on a cluster with Compaq Alpha ES40 (4 × 833 MHz) processors, and Gaussian 03W revision B.03[20] on a personal computer with a Pentium 4, 2.8 GHz processor. Calculations used all Gaussian defaults (unless noted otherwise) except that the Gaussian overlay option IOP(3/32 = 2) was used in all calculations to prevent the reduction of expansion sets. All of the calculations were carried out using SCF=Tight to ensure proper SCF convergence, which is especially important if meaningful results are to be obtained where a basis set contains diffuse functions.

Representative zero-point vibrational energy corrections for the molecules studied in this paper were found to change the relative conformer energies (including the barriers to internal rotation) by less than 5%. The ab initio relative energies and barriers to internal rotation presented in this paper have not been scaled, and zero point energies have been neglected.

Results and Discussion

Properties of the Model $M(CH_3)_4$ System. Our model for investigating the nature of site−site potentials is the $M(CH_3)_4$ system. By varying both the displacements of the CH oscillators and the H-C-*M*-C dihedral angle, ϕ, on two methyl rotors we are able to interrogate a broad range of d_{HH} values. We assume an adiabatic separation between stretching and torsional motions, that is, we will consider the stretching states of various torsional states, ϕ. Varying the central atom, *M*, enables us to explore whether intramolecular site−site potentials are transferable between molecules. Specifically, we investigate site−site potentials in the $M(CH_3)_4$ system where M = C (neopentane) and M = Si (TMS). For both molecules, the minimum energy conformation occurs when the dihedral angle of each methyl rotor is $\phi = 60°$ with respect to the MC_4 framework.

Changes in the energy of an $M(CH_3)_4$ homologue are explored along two torsional coordinates, ϕ, and two CH stretch coordinates, *q*. The two stretch coordinates are the closest CH bonds located on different methyl groups. Displacements along these local stretch coordinates are referred to as local mode displacement, q_L, and "crowding" (local mode) displacement, q_C. The hydrogen atoms associated with these two displacements are denoted H_L and H_C, respectively. The two torsional coordinates are the dihedral angle H_L-C-*M*-C, denoted ϕ_L, and the dihedral angle H_C-C-*M*-C, denoted ϕ_C.

Because of the geometry of $M(CH_3)_4$ systems, H_L will interact strongly with one or at most two different hydrogen atoms, depending upon the values of ϕ_L and ϕ_C. Where ϕ_L and ϕ_C approach 60°, H_L can interact with H_C and another proximal atom, $H_{C'}$. As ϕ_L and ϕ_C approach 0°, significant interactions of H_L occur only with the most proximal atom, H_C.

TABLE 1: Ab Initio Relative Energies[a] and Bond Lengths of a Variety of Conformations of Neopentane and TMS

molecule	theory/ basis set[b]	conformer (ϕ_L,ϕ_C)	ΔE (cm^{-1})	Δr_e ($\times 10^{-3}$ Å) CH_L	Δr_e ($\times 10^{-3}$ Å) CH_C
neopentane	(1)	0°, 0°	3160	−2.88	−2.89
		0°, 60°	1430	−1.30	0.14
		60°, 0°	1430	0.14	−1.30
		60°, 60°	0	0.00	0.00
	(2)	0°, 0°	2730	−2.45	−2.45
		0°, 60°	1270	−1.34	0.01
		60°, 0°	1270	−0.14	−1.32
		60°, 60°	0	0.00	0.00
TMS	(1)	0°, 0°	1250	−1.25	−1.26
		0°, 60°	580	−0.75	0.12
		60°, 0°	580	0.12	−0.75
		60°, 60°	0	0.00	0.00
	(2)	0°, 0°	1030	−0.94	−0.92
		0°, 60°	480	−0.64	0.09
		60°, 0°	480	0.02	−0.76
		60°, 60°	0	0.00	0.00

[a] Relative to the lowest energy ($\phi_L = \phi_C = 60°$) conformer. Energies not scaled. [b] (1) denotes HF/6-311++G(2d,2p), whereas (2) denotes B3LYP/cc-pVTZ.

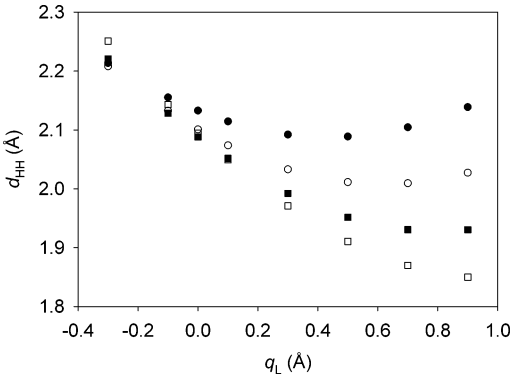

Figure 1. The relationship between q_L and d_{HH} for the $\phi_L = \phi_C = 0°$ conformer of neopentane at $q_C = 0.00$ Å (solid circle), $q_C = 0.20$ Å (hollow circle), $q_C = 0.40$ Å (solid square), and $q_C = 0.60$ Å (hollow square) calculated at HF/6-311++G(2d,2p).

The H_L and H_C oscillators couple with methyl torsional modes. Changes in H_L and H_C bond lengths with changes in torsional angles ϕ_L and ϕ_C in neopentane and TMS are presented in Table 1. CH bond lengths are shorter in the $\phi_L = \phi_C = 0°$ conformer than in the $\phi_L = \phi_C = 60°$ conformer for both neopentane and TMS. The magnitude of CH bond contraction at $\phi_L = \phi_C = 0°$ is greater in neopentane than in TMS, indicating (1) a stronger stretch-torsion coupling[1] and (2) a greater barrier to high amplitude stretching motion in neopentane as compared to TMS. Effects are being transmitted through-space to nonadjacent bonds.

Neopentane, $C(CH_3)_4$. In the equilibrium conformation ($\phi_L = \phi_C = 60°$, $q_L = q_C = 0.00$ Å) the separation between H_L and H_C (or $H_{C'}$) is $d_{HH} = 256$ pm.[21] Taking the van der Waals radius for hydrogen to be 120 pm,[22] the separation of van der Waals spheres for hydrogen, δ_{HH}, is 16 pm.[21]

The separation, d_{HH}, is modulated by variables ϕ_L, ϕ_C, q_L, and q_C. In the $\phi_L = \phi_C = 0°$ conformer of neopentane, the distance between nearest hydrogens is 214 pm at $q_L = q_C = 0.00$ Å (see Figure 1). If we allow q_L to vary from −0.30 to 0.90 Å and q_C to vary from 0.00 to 0.60 Å (vide infra), then the range of d_{HH} values investigated in the $\phi_L = \phi_C = 0°$ conformer of neopentane is 185 to 225 pm. At a given q_C, there are often two different displacements, q_L, that can lead to the same internuclear distance, d_{HH} (consider the $\phi_L = \phi_C = 0°$, $q_C = 0.00$ Å conformer where $q_L = 0.60$ Å and $q_L \simeq 0.28$ Å both lead to the same d_{HH}). A site−site potential expressed as a function of d_{HH} therefore need not be single-valued.

Because of the very short d_{HH} separations in neopentane, through-space coupling is strong. This coupling facilitates IVR and leads to very short vibrational overtone lifetimes. These lifetimes range from 110 fs for the second overtone to approximately 40 fs for high overtones.[21]

TMS, $Si(CH_3)_4$. The SiC bond in TMS is longer than the CC bond in neopentane. The equilibrium value of d_{HH} (i.e., at $\phi_L = \phi_C = 60°$, $q_L = q_C = 0.00$ Å) is 313 pm.[21] The separation of the van der Waals spheres for hydrogen, δ_{HH}, is 73 pm.[21] This greater δ_{HH} separation leads to weaker through-space coupling in TMS (as compared to neopentane). This weaker coupling is born out by the longer, nearly constant CH overtone lifetimes of 150 ± 30 fs.[21]

As in neopentane, the separation, d_{HH}, is modulated by variables ϕ_L, ϕ_C, q_L, and q_C. In TMS, the modulation of d_{HH} as a function of q_L and q_C in the $\phi_L = \phi_C = 0°$ conformation is qualitatively similar to that of neopentane (vide supra), except for larger d_{HH} separations that range from 235 to 272 pm.

Through-Space Interactions. The stretching potential of a molecule, V_S, is approximately separable along local modes.[23] For a molecule with local mode oscillator L, a proximal, nonbonded, crowding local mode oscillator, C, and remaining local modes, *i*, we write

$$V_S = V_L + V_C + \sum V_i \tag{8}$$

The stretching potential of individual local mode oscillators are the sum of their unperturbed potentials, $V_{L,0}(q_L)$, plus nonbonded (through-space) perturbations arising from interactions with H_C and (possibly) $H_{C'}$

$$V_L(q_L) = V_{L,0}(q_L) + V_{L,nb}(d_{LC}) + V_{L,nb}(d_{LC'}) \tag{9}$$

where the individual terms are all at the same specific conformation described by parameters ϕ_L and ϕ_C. Note that the unperturbed CH stretching potential is expressed naturally in terms of displacements from equilibrium, q_L, and the nonbonded interactions between atoms H_L and H_C are best expressed in terms of the internuclear distance, *d*, which separates these atoms. We simplify the potential $V_L(q_L)$ by introducing the condition

$$V_{L,nb}(d_{LC'}) = 0 \tag{10}$$

which holds if $\phi_L = \phi_C = 0°$ and becomes increasingly incorrect as we approach the limit $\phi_L,\phi_C \rightarrow 60°$.

The strongest through-space interaction with H_L occurs in the sterically crowded $\phi_L = \phi_C = 0°$ conformer. We restrict the scope of our inquiry to this conformer and simplify the notation somewhat by denoting $V_{L,nb}(d_{LC})$ as $V_{nb}(d_{HH})$. Equation 9 becomes

$$V_{nb}(d_{HH}) = V_L(q_L) - V_{L,0}(q_L) \tag{11}$$

Thus, the nonbonded site−site potential between two proximal hydrogen atoms on different methyl groups, $V_{nb}(d_{HH})$, can be obtained by subtracting the unperturbed ab initio potential energy surface, $V_{L,0}(q_L)$, from the perturbed ab initio potential energy surface, $V_L(q_L)$. The unperturbed potential $V_{L,0}(q_L)$ is that in which one CH bond is successively displaced from equilibrium to map out the potential energy surface, where all other geometric parameters (including the bond CH_C) are constrained to their equilibrium values. The perturbed potential, $V_L(q_L)$, is identical to $V_{L,0}(q_L)$ except that the CH_C bond has been displaced

from its equilibrium value. This CH_C bond, which is proximal to CH_L (through space) but attached to a different methyl group than CH_L, crowds the CH_L stretching potential at positive bond displacements, introducing a nonbonded site−site interaction.

As mentioned previously, the ab initio potentials presented in this paper are not scaled, and zero point energies are not corrected for.

Distributions Over Molecular Conformations. Experimental results that depend on molecular conformation yield an average over a distribution of conformations. For example, the lowest-energy conformers of neopentane and TMS have all four methyl groups staggered with respect to the molecular MC_4 skeleton. In this case the H-C-*M*-C dihedral angle, ϕ, is 60 °. Quantum mechanically, the observed dihedral angle is given by the ensemble average over quantum states of the expectation value, $\langle\phi\rangle$. However, the standard deviation in ϕ values can be substantial. Denoting this standard deviation by σ_ϕ, we express this quantity as[24]

$$\sigma_\phi = \sqrt{\langle\phi^2\rangle - \langle\phi\rangle^2} \tag{12}$$

where

$$\langle\phi^n\rangle = \langle\psi|\phi^n|\psi\rangle \tag{13}$$

The torsional wavefunction, ψ, is a normalized ensemble average of the wavefunctions that are significantly populated at temperature *T*.

The evaluation of eq 12 was expedited by using torsional wavefunctions composed of symmetry-adapted basis states. The potentials for internal CH_3 rotation in both neopentane and TMS possess C_{3v} symmetry. Symmetry-adapted basis functions of symmetry Γ, $|\chi_m^\Gamma\rangle$, were made from the projection of the free rotor eigenfunction, $e^{im\phi}$, on the A_1, A_2, and E irreducible representations.[21] These orthogonal basis functions were normalized, allowing us to expand eq 13 to

$$\langle\phi^n\rangle = \frac{\langle\phi^n\rangle^{A_1} + \langle\phi^n\rangle^{A_2} + \langle\phi^n\rangle^{E}}{\sum_j e^{-\beta E_j^{A_1}} + \sum_j e^{-\beta E_j^{A_2}} + \sum_j e^{-\beta E_j^{E}}} \tag{14}$$

where $\beta = (kT)^{-1}$. The expectation value of the irreducible representation, Γ, is

$$\langle\phi^n\rangle^\Gamma = \sum_j^{N_\Gamma} e^{-\beta E_j^\Gamma} \sum_m c_{j,m}^* \; c_{j,m} \langle\chi_m^\Gamma|\phi^n|\chi_m^\Gamma\rangle \tag{15}$$

where the expansion coefficients, $c_{j,m}$, were obtained by diagonalizing the Hamiltonian[21] of the torsional wavefunctions of energy *j*, expanded in N_Γ terms of basis states $|\chi_m^\Gamma\rangle$ (where *m* is an index). The normalized symmetry adapted basis functions were, respectively

$$|\chi_m^{A_1}\rangle = \frac{\cos(m\phi)}{\sqrt{\pi(1+\delta_m)}} \text{ when } m = 0, 3, 6, \ldots$$
$$= 0 \qquad \text{otherwise} \tag{16}$$

$$|\chi_m^{A_2}\rangle = \frac{\sin(m\phi)}{\sqrt{\pi}} \text{ when } m = 3, 6, 9, \ldots$$
$$= 0 \qquad \text{otherwise} \tag{17}$$

and

$$|\chi_m^{E}\rangle = \frac{e^{im\phi}}{\sqrt{2\pi}} \text{ when } m = \pm1, \pm2, \pm4, \pm5, \pm7, \pm8, \ldots$$
$$= 0 \qquad \text{otherwise.} \tag{18}$$

Scope of Inquiry. Having determined that changes in ϕ_L and ϕ_C have effects (transmitted through-space) on the equilibrium carbon−hydrogen bond lengths and on the barrier to internal methyl rotation (vide supra and Table 1), the scope of inquiry of this paper is the following: (1) Determine the standard deviation in the dihedral angle ϕ (using eq 12) in neopentane and TMS to ascertain whether it is reasonable to consider $\phi_L = \phi_C = 0°$ conformers. (2) Calculate the nonbonded site−site potential between proximal hydrogen atoms on different carbon atoms, $V_{nb}(d_{HH})$, using eq 11 and ab initio data. What are the relative contributions of the numerous electrostatic terms to the nonbonded site−site potential? (3) Obtain ab initio $\tilde{\omega}$ and $\tilde{\omega}x$ from fits of potential energy surfaces calculated at different conformations to a Morse potential (eq 1). (4) Ascertain whether the Morse potential is a good basis in which to expand $V_{nb}(d_{HH})$. This will be investigated by carrying out a fit of ab initio potential energy surfaces, calculated at various q_C, ϕ_L, and ϕ_C (i.e., under various degrees of through-space perturbation) to a Morse potential (eq 1) and to a generalized Morse potential (eq 2), paying particular attention to the effect of steric crowding on standard deviations in the fit to Morse potentials.

The potential energy surfaces of neopentane and TMS were calculated with respect to four degrees of freedom: q_L, q_C, ϕ_L, and ϕ_C. Values of q_L ranged from −0.30 Å to 0.90 Å in steps of 0.10 Å, whereas q_C values ranged from 0.00 to 0.60 Å in steps of 0.10 Å. Torsional angles ϕ_L and ϕ_C were both varied from 0° to 60° in steps of 10°. The resulting grid size is $7 \times 7 \times 7 \times 13$, which corresponds to 4459 ab initio calculations for each molecule. Ab initio calculations were carried out at HF/6-31G(d,p), HF/6-311++G(2d,2p), B3LYP/cc-pVDZ, and B3LYP/cc-pVTZ.

Charge Distribution. Charge distribution within a molecule is too anisotropic to be modeled by any single set of atom-centered charges unless one is concerned only with long-distance interactions.[25] Charge distribution calculations will therefore not be used to investigate contributions to $V_{nb}(d_{HH})$ quantitatively; however, because electrostatic terms are very important in nonbonded interactions,[26] charge distribution calculations will be used to qualitatively illustrate the nature of electrostatic contributions to $V_{nb}(d_{HH})$. Specifically, we will use CHelpG,[27] which is suitable for nonbonded interactions at long distances,[25] to visualize molecular isosurfaces in various $M(CH_3)_4$ conformations. CHelpG is a grid-based method in which atomic and molecular charges are fitted to reproduce the expectation value of the molecular electrostatic potential at the van der Waals surface.[28]

Limitations on the Concept of Dihedral Angle. In a previous paper,[1] it was determined that B3LYP/cc-pVDZ adequately treated nonbonded interactions as it led to excellent scaled frequencies for the normal modes of vibration in sterically crowded molecules such as neopentane. The B3LYP/cc-pVDZ geometries of neopentane and TMS were used to determine the projection of the moment of inertia along the axis of internal rotation, *I*. These values are presented in Table 2, along with the barriers to internal rotation.

The torsional wavefunctions of A_1, A_2, and E symmetry were determined by diagonalizing the rigid rotor Hamiltonian in a threefold potential[21] using basis functions $|\chi_m^{A_1}\rangle$ (eq 16), $|\chi_m^{A_2}\rangle$

TABLE 2: Expectation Values of the Dihedral Angles and Their Standard Deviations

molecule	barrier (cm^{-1})[a]	I (kg m^2)	$\langle\phi\rangle \pm \sigma_\phi$ (deg)
neopentane	1330	5.31×10^{-47}	60 ± 13.7
TMS	520	5.20×10^{-47}	60 ± 22.0

[a] Barriers to internal methyl rotation calculated at B3LYP/cc-pVDZ.

TABLE 3: Expectation Values of the Dihedral Angles,[a] their Standard Deviations, and the Relative Populations of the Torsional Wavefunctions of Neopentane at 298 K

wavefunction	symmetry	$\langle\phi\rangle$ (deg)	σ_ϕ(deg)	P_{rel}
Φ_0	A_1	60	8.5	0.55360
Φ_1	A_1	60	20	0.05905
Φ_2	A_1	60	29	0.00849
Φ_3	A_1	60	43	0.00209
Φ_4	A_1	60	43	0.00068
Φ_5	A_1	60	38	0.00010
Φ_{ave}	A_1	60	10	
Φ_0	A_2	60	15	0.17501
Φ_1	A_2	60	25	0.02142
Φ_2	A_2	60	33	0.00361
Φ_3	A_2	60	38	0.00072
Φ_4	A_2	60	38	0.00010
Φ_{ave}	A_2	60	16	
Φ_0	E	60	14	0.27756
Φ_1	E	60	15	0.22454
Φ_2	E	60	24	0.04182
Φ_3	E	60	25	0.03049
Φ_4	E	60	33	0.00782
Φ_5	E	60	34	0.00543
Φ_6	E	60	39	0.00192
Φ_7	E	60	39	0.00122
Φ_8	E	60	39	0.00040
Φ_9	E	60	38	0.00021
Φ_{ave}	E	60	17	
Φ_{ave}	all	60	14	

[a] Calculated using the parameters in Table 2.

(eq 17), and $|\chi_m^E\rangle$ (eq 18), respectively. These torsional wavefunctions are denoted ψ_{A_1}, ψ_{A_2}, and ψ_E. The ψ_E torsional wavefunction was composed of 60 basis functions, $|\chi_m^E\rangle$ where $m = 1, 2, 4, 5, ..., 89$. Both ψ_{A_1} and ψ_{A_2} are composed of 30 basis functions (i.e., $m = 0, 3, 6, ... 87$ for ψ_{A_1} and $m = 3, 6, 9, ..., 90$ for ψ_{A_2}).

Approximately 49 wavefunctions of A_1, A_2, and E symmetry were significantly populated at 298 K for neopentane and TMS. These wavefunctions are used to calculate the expectation value of the dihedral angle, $\langle\phi\rangle$ (eq 12), the uncertainty in ϕ, σ_ϕ (eq 13), and, using eqs 15, the ensemble average values of $\langle\phi\rangle$ and σ_ϕ. The ensemble averages are given in Table 2. Details of the individual contributions to the ensemble are presented for neopentane (Table 3) and TMS (Table 4).

The relative probability distribution, $\psi^*\psi$, of an ensemble of quantized hindered rotors at 298 K was calculated for neopentane and TMS. This distribution is shown in Figure 2. The barriers to internal rotation were modeled as $\cos^2(3\phi/2)$ functions. Physical parameters were calculated at the B3LYP/cc-pVDZ level of theory and basis set (see Table 2). The neopentane and TMS distributions were averaged over 14 rotational energy levels of A_1 and A_2 symmetry and 25 rotational energy levels of E symmetry. Distributions were normalized over the interval $[0, 2\pi]$. The large σ_ϕ value in TMS (Table 2) and broad $\psi^*\psi$ distribution (Figure 2) indicate that all methyl torsional conformations are significantly populated at 298 K. Although this distribution is somewhat narrower in neopentane than in TMS, it still seems appropriate to consider nonequilibrium conformations (such as $\phi_L = \phi_C = 0°$ in $M(CH_3)_4$ systems) when investigating $V_{nb}(d_{HH})$.

TABLE 4: Expectation Values of the Dihedral Angles,[a] their Standard Deviations, and the Relative Populations of the Torsional Wavefunctions of TMS at 298 K

wavefunction	symmetry	$\langle\phi\rangle$ (deg)	σ_ϕ(deg)	P_{rel}
Φ_0	A_1	60	11	0.69205
Φ_1	A_1	60	30	0.18416
Φ_2	A_1	60	45	0.07956
Φ_3	A_1	60	40	0.03120
Φ_4	A_1	60	37	0.00638
Φ_5	A_1	60	36	0.00079
Φ_{ave}	A_1	60	18	
Φ_0	A_2	60	20	0.34270
Φ_1	A_2	60	32	0.10285
Φ_2	A_2	60	37	0.03151
Φ_3	A_2	60	36	0.00638
Φ_4	A_2	60	36	0.00079
Φ_{ave}	A_2	60	24	
Φ_0	E	60	19	0.48361
Φ_1	E	60	20	0.41484
Φ_2	E	60	32	0.17003
Φ_3	E	60	33	0.13554
Φ_4	E	60	39	0.06814
Φ_5	E	60	38	0.04781
Φ_6	E	60	37	0.01953
Φ_7	E	60	37	0.01148
Φ_8	E	60	36	0.00336
Φ_9	E	60	36	0.00167
Φ_{10}	E	60	36	0.00035
Φ_{11}	E	60	36	0.00015
Φ_{ave}	E	60	24	
Φ_{ave}	all	60	22	

[a] Calculated using the parameters in Table 2.

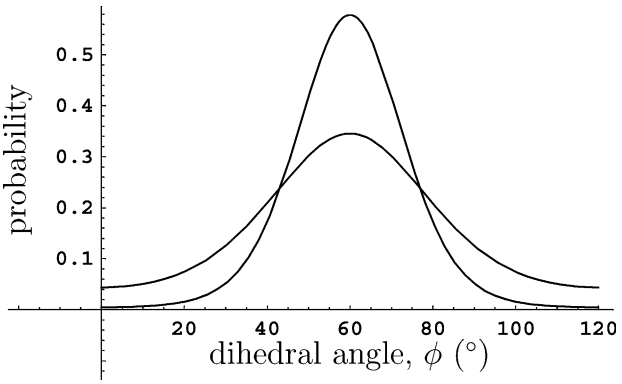

Figure 2. Relative probability distributions for an ensemble of methyl rigid rotors in neopentane and TMS modeled as a $\cos^2(3\phi/2)$ function. The neopentane distribution is the sharper of the two.

Wavefunction Stability. Ab initio wavefunction stability eigenvalues depend on the level of theory and basis set. They were also found to be sensitive to molecular conformation, both in terms of dihedral angle and in terms of bond displacements (from equilibrium). Eigenvalues decrease (i.e., the ab initio wavefunction becomes more unstable) with increasing displacement from the equilibrium bond length, r_e. Simultaneous displacements along q_L and q_C lead to a negligibly small increase in wavefunction instability over that caused by stretching along a single coordinate. All ab initio calculations used in this paper are restricted to conformations where the ab initio wavefunctions are stable. The data domain was restricted to CH displacements in [−0.30, 0.50] Å for HF/6-311++G(2d,2p) and to [−0.30, 0.70] Å for B3LYP/cc-pVTZ. Unless noted otherwise, data that are presented graphically are rendered in CH displacement step sizes of 0.20 Å.

Through-Space Interactions. There are two complementary ways of visualizing nonbonded, site−site potentials, $V_{nb}(d_{HH})$ (eq 11). One is to plot the site−site potential as a function of

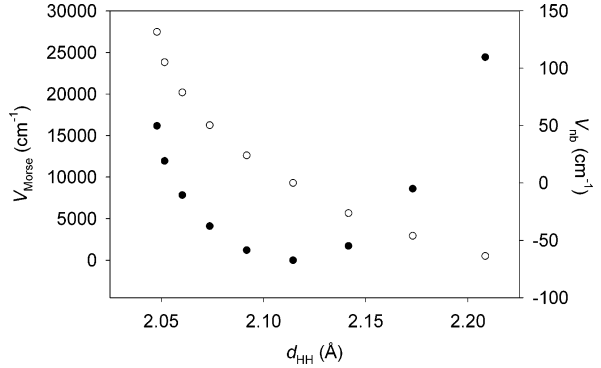

Figure 3. Unscaled ab initio potential, $V(d_{HH})$, (solid) and nonbonded potential, $V_{nb}(d_{HH})|_{qC}$ (empty), for the $\phi_L = \phi_C = 0°$, $q_C = 0.10$ Å conformer of neopentane calculated at HF theory using the 6-311++G-(2d,2p) basis set. The q_L step size is 0.10 Å.

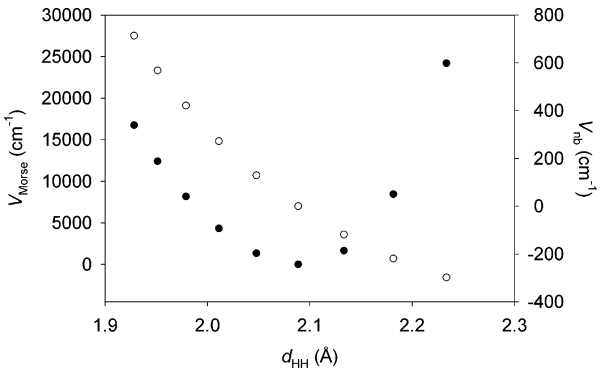

Figure 4. Unscaled ab initio potential, $V(d_{HH})$, (solid) and nonbonded potential, $V_{nb}(d_{HH})|_{qC}$, (empty) for the $\phi_L = \phi_C = 0°$, $q_C = 0.50$ Å conformer of neopentane calculated at HF theory using the 6-311++G-(2d,2p) basis set. The q_L step size is 0.10 Å.

d_{HH} where the values of q_C, ϕ_L, and ϕ_C are held constant. The potential is first calculated as a function of q_L, and then a coordinate transformation is carried out to give the potential in terms of d_{HH}. This form of potential, done at constant q_C, will be denoted $V_{nb}(d_{HH})|_{qC}$. The other representation is the site−site potential as a function of d_{HH} where both q_L and q_C are variables and the values of ϕ_L and ϕ_C are held constant. This plot of H···H interactions is denoted $V_{nb}(d_{HH})|_{allq}$. Note that site−site potentials expressed as functions of d_{HH} will be well-behaved only if we can reasonably approximate their dependencies on q_L and q_C by a single variable, d_{HH}.

Plots of the unscaled HF/6-311++G(2d,2p) potential, $V(d_{HH})$, and nonbonded potential, $V_{nb}(d_{HH})|_{qC}$, in neopentane are presented for the $\phi_L = \phi_C = 0°$, $q_C = 0.10$ Å conformer and the $\phi_L = \phi_C = 0°$, $q_C = 0.50$ Å conformer in Figures 3 and 4, respectively. In both figures, the potentials, $V(d_{HH})$, appear vaguely Morse-like, despite the transformation from q_L space to d_{HH} space, that is, from the CH stretching potential as a function of bond displacement to CH stretching potential as a function of internuclear separation, d_{HH}. The nonbonded potential, $V_{nb}(d_{HH})|_{qC}$, is approximately linear in d_{HH}, especially for the more sterically hindered conformer (Figure 4). Steric interactions are stronger in the (more crowded) $\phi_L = \phi_C = 0°$, $q_C = 0.50$ Å conformer than in the $\phi_L = \phi_C = 0°$, $q_C = 0.10$ Å conformer. It is interesting that $V_{nb}(d_{HH})|_{qC}$ is not Morse or Lennard−Jones like. Corresponding plots for neopentane calculated at B3LYP/cc-pVTZ, as well as those for TMS calculated at both HF/6-311++G(2d,2p) and B3LYP/cc-pVTZ, are qualitatively similar and are not presented in this paper. We conclude that it is possible to express $V_{nb}(d_{HH})|_{qC}$ in terms of a single variable, d_{HH}, because $V_{nb}(d_{HH})|_{qC}$ is well-behaved and single-

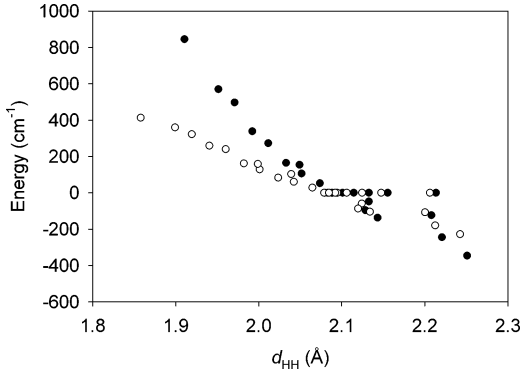

Figure 5. Unscaled site−site potential for all q_L and q_C, $V_{nb}(d_{HH})|_{allq}$, of the $\phi_L = \phi_C = 0°$ conformer of neopentane calculated at HF/6-311++G(2d,2p) (solid) and B3LYP/cc-pVTZ (hollow).

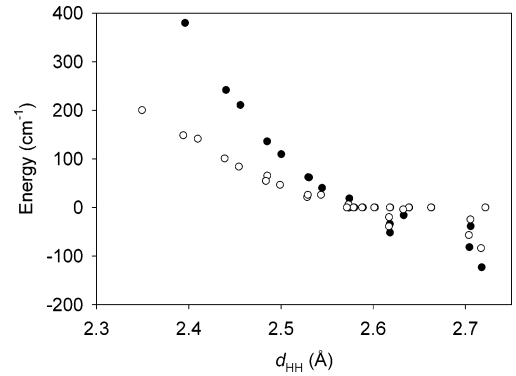

Figure 6. Unscaled site−site potential $V_{nb}(d_{HH})|_{allq}$ of the $\phi_L = \phi_C = 0°$ conformer of TMS calculated at HF/6-311++G(2d,2p) (solid) and B3LYP/cc-pVTZ (hollow).

valued over the range of $\phi_L = \phi_C = 0°$ conformers despite the fact that the linear transformation of q_L is not *onto* d_{HH} (Figure 1).

The more general potential $V_{nb}(d_{HH})|_{allq}$ (i.e., $V_{nb}(d_{HH})$ expressed as a function of d_{HH} where q_L and q_C are variables) at the $\phi_L = \phi_C = 0°$ conformers of neopentane and TMS was calculated at both HF/6-311++G(2d,2p) and B3LYP/cc-pVTZ and is presented in Figures 5 and 6. The domain of the HF/6-311++G(2d,2p) data is less than that of the B3LYP/cc-pVTZ data (i.e., q_L, $q_C \in [-0.30, 0.50]$ Å versus q_L, $q_C \in [-0.30, 0.70]$ Å) in order to ensure that the ab initio wavefunction is stable. In all cases, there is a decrease in $V_{nb}(d_{HH})|_{allq}$ with increasing d_{HH}, which appears to be approximately linear over the regions of d_{HH} space studied. This linearity indicates that it is reasonable to express $V_{nb}(d_{HH})|_{allq}$, calculated as a function of both q_L and q_C, in terms of a single variable, d_{HH}.

The conditions assumed in the derivation of eq 11 were tested by plotting $V_{nb}(d_{HH})|_{allq}$ for the $\phi_L = \phi_C = 10°$ and $\phi_L = \phi_C = 20°$ conformers of neopentane and TMS and comparing these plots to those obtained for the $\phi_L = \phi_C = 0°$ conformers. In this manner, we test the effect of the condition in eq 10 where we restrict ourselves to eclipsed conformers, simplifying the potential $V_{nb}(d_{HH})$ to one between at most two hydrogen atoms. It was found that the plots of $V_{nb}(d_{HH})|_{allq}$ for the $\phi_L = \phi_C = 10°$ and $\phi_L = \phi_C = 20°$ conformers (which are not shown) are virtually identical to one another. These plots are very similar to those at $\phi_L = \phi_C = 0°$, except that the former have been shifted approximately 60 cm^{-1} higher in energy at B3LYP/cc-pVTZ in neopentane and 30 cm^{-1} higher in energy at B3LYP/cc-pVTZ in TMS. The energy increase is caused by an augmentation to interactions between H_L and H_C by $H_{C'}$. The additional interaction of the third hydrogen is not negligible

and obfuscates the nature of the potential $V_{nb}(d_{HH})|_{allq}$. We therefore restrict our investigations to $\phi_L = \phi_C = 0°$ conformers.

To determine whether it is possible to obtain a conformation-*independent* site−site potential, we overlaid plots of $V_{nb}(d_{HH})|_{allq}$ at various ϕ_L and ϕ_C. The resulting figures (which are not presented) were discontinuous and poorly behaved for both neopentane and TMS at all combinations of theory and basis set, indicating that conformation-independent site−site potentials cannot be expressed as functions of d_{HH}. The potential $V_{nb}(d_{HH})|_{allq}$ as a function of d_{HH} is specific to calculation level and basis set, to molecular conformation, and to a given molecule.

The slope of $V_{nb}(d_{HH})|_{allq}$ in neopentane (Figure 5) is always negative, indicating that the through-space potential between proximal hydrogens is always repulsive (for the conformers studied), even at large d_{HH}. This repulsive nature of $V_{nb}(d_{HH})|_{allq}$ in neopentane is likely caused by strong C−C and C−H bonds forcing the H_L and H_C hydrogens into closer proximity than the sum of their van der Waals radii.

In Figure 5, we note that the uncorrelated $V_{nb}(d_{HH})|_{allq}$ values calculated at HF/6-311++G(2d,2p) for the $\phi_L = \phi_C = 0°$ conformer of neopentane increase more rapidly with decreasing d_{HH} than do the correlated B3LYP/cc-pVTZ values. Both the correlated and uncorrelated $V_{nb}(d_{HH})|_{allq}$ values are not scaled, however, based on the similarity of the HF/6-311++G(2d,2p) and B3LYP/cc-pVTZ local mode scaling factors (vide infra) the disparity between the two sets of $V_{nb}(d_{HH})|_{allq}$ values cannot be ascribed to the omission of scaling. Rather, the disparity indicates that it is important to include electron correlation in the calculation of $V_{nb}(d_{HH})$, especially at small values of d_{HH}, where electron correlation effects are pronounced. At small d_{HH}, the slope of the uncorrelated site−site potential is approximately -4000 cm^{-1}/Å, whereas that of the correlated site−site potential is approximately -2000 cm^{-1}/Å.

The potential $V_{nb}(d_{HH})|_{allq}$ appears to be well-described by d_{HH} at small values of d_{HH}. At large d_{HH}, there appears to be an oscillatory component where $V_{nb}(d_{HH})|_{allq}$ is double-valued. This is especially apparent at large d_{HH} in the B3LYP/cc-pVTZ calculated values of $V_{nb}(d_{HH})|_{allq}$ in TMS (Figure 6). The presence of overlaid "shingles" in $V_{nb}(d_{HH})|_{allq}$ is caused because, depending on the values of q_C, ϕ_L, and ϕ_C, there can be two different values of q_L that have the same d_{HH} (vide supra). In cases where $V_{nb}(d_{HH})|_{allq}$ appears to be double-valued, the higher values of $V_{nb}(d_{HH})|_{allq}$ arise from the conformers where $|q_C| < |q_L|$.

Steric interactions in the $\phi_L = \phi_C = 0°$ conformer of TMS are weaker than those of the same conformer in neopentane. The nonbonded site−site potential of TMS, $V_{nb}(d_{HH})$, (Figure 6) is linear in d_{HH} and approximately half of that in neopentane (Figure 5). At small d_{HH}, the slope of the uncorrelated site−site potential is approximately -2000 cm^{-1}/Å, whereas that of the correlated site−site potential is approximately -1000 cm^{-1}/Å.

With the *caveat* that the values of $V_{nb}(d_{HH})|_{allq}$ in this paper have not been scaled, it is apparent that (1) electron correlation contributes significantly to nonbonded, site−site potentials in neopentane and TMS, accounting for nearly half of the through-space interaction, and (2) $V_{nb}(d_{HH})|_{allq}$ in TMS is approximately half of that in neopentane.

One unexpected result in this paper is that potential $V_{nb}(d_{HH})|_{allq}$ is repulsive even at large d_{HH} in TMS (Figure 6) where d_{HH} is greater than the sum of two hydrogen van der Waals radii. The very existence of van der Waals radii indicates that nonbonded atoms are attractive at long ranges. Such attractions

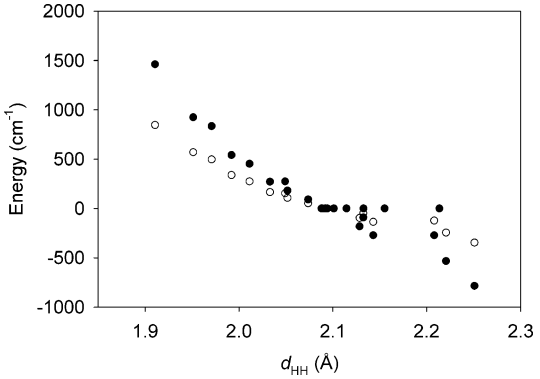

Figure 7. Site−site potential for all q_L and q_C of the $\phi_L = \phi_C = 0°$ conformer of neopentane, $V_{nb}(d_{HH})|_{allq}$ (hollow), and the kinetic energy contribution to this potential, $T_{nb}(d_{HH})$ (solid), calculated at HF/6-311++G(2d,2p).

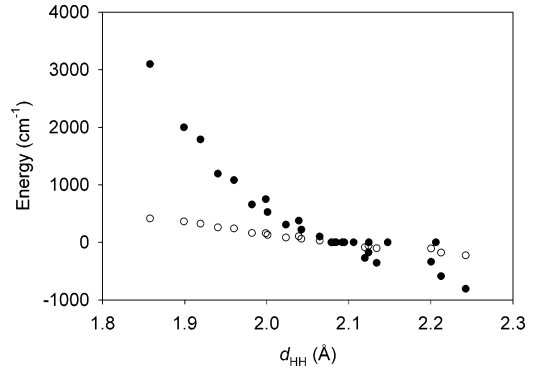

Figure 8. Site−site potential for all q_L and q_C of the $\phi_L = \phi_C = 0°$ conformer of neopentane, $V_{nb}(d_{HH})|_{allq}$ (hollow), and the kinetic energy contribution to this potential, $T_{nb}(d_{HH})$ (solid), calculated at B3LYP/cc-pVTZ.

are often modeled with Lennard−Jones functions. The nonbonded site−site potentials for neopentane and TMS are decidedly non-Lennard−Jones-like (Figures 3−6). One would expect that the nonbonded site−site potential between H_L and H_C would become attractive when $d_{HH} > \sum r_{vdW}$. Representative values of $V_{nb}(d_{HH})$ were calculated at the MP2 level of theory with a 6-31G(d,p) basis set for neopentane and TMS. The explicit inclusion of electron correlation led to results similar to those obtained at the HF and B3LYP levels of theory in which $V_{nb}(d_{HH})|_{allq}$ is repulsive at all d_{HH}.

A cut-plane of the electrostatic potential (EP) from the B3LYP Kohn−Sham density in neopentane for the $\phi_L = \phi_C = 0°$, $q_L = 0.60$ Å, $q_C = 0.30$ Å conformer indicates that there are decreases in electron density about the hydrogen atoms associated with stretches along the CH bond. Changes in electron density and EP can also be visualized using isosurfaces. The isosurface of the $\phi_L = \phi_C = 0°$, $q_L = 0.60$ Å, $q_C = 0.00$ Å conformer of neopentane shows the EP becoming more negative along the CH bond axis as that bond stretches. To understand why the $H_L\cdots H_C$ interaction is repulsive at large d_{HH}, we will investigate the contributions to through-space interactions of the individual energy terms.

Contributions to $V_{nb}(d_{HH})$ were calculated from expressions of the form of eq 11. These contributions to $V_{nb}(d_{HH})$ are kinetic energy, $T_{nb}(d_{HH})$, electron−electron potential, $V_{nb,ee}(d_{HH})$, nuclear−nuclear potential, $V_{nb,NN}(d_{HH})$, and electron−nuclear potential, $V_{nb,eN}(d_{HH})$.

The kinetic energy contribution to $V_{nb}(d_{HH})|_{allq}$ becomes increasingly negative with increasing d_{HH} in both neopentane (Figures 7 and 8) and TMS (Figures 9 and 10). The magnitude of $T_{nb}(d_{HH})$ is comparable to that of $V_{nb}(d_{HH})|_{allq}$, especially for

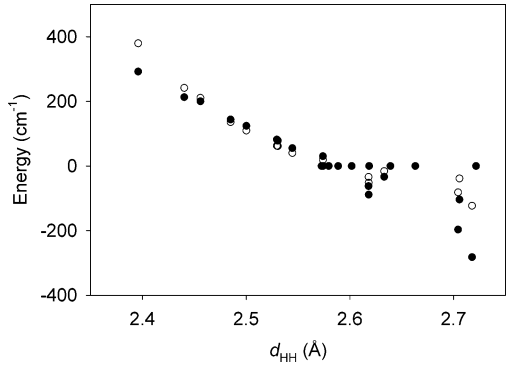

Figure 9. Site−site potential for all q_L and q_C of the $\phi_L = \phi_C = 0°$ conformer of TMS, $V_{nb}(d_{HH})|_{allq}$ (hollow), and the kinetic energy contribution to this potential, $T_{nb}(d_{HH})$ (solid), calculated at HF/6-311++G(2d,2p).

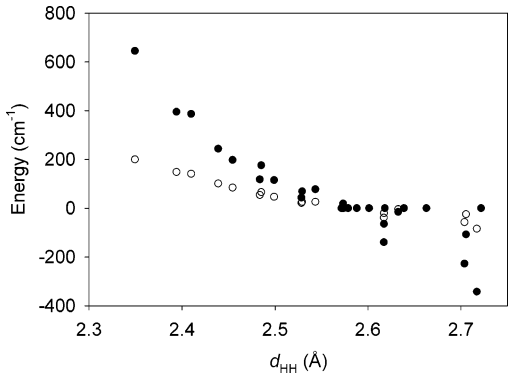

Figure 10. Site−site potential for all q_L and q_C of the $\phi_L = \phi_C = 0°$ conformer of TMS, $V_{nb}(d_{HH})|_{allq}$ (hollow), and the kinetic energy contribution to this potential, $T_{nb}(d_{HH})$ (solid), calculated at B3LYP/cc-pVTZ.

uncorrelated calculations carried out at small d_{HH}. Correlated calculations predicted larger $T_{nb}(d_{HH})$ contributions than uncorrelated calculations. Note that the data domains of the correlated and uncorrelated calculations were restricted to regions where the ab initio wavefunction is stable. At large and small d_{HH}, the magnitude of the contribution of $T_{nb}(d_{HH})$ to $V_{nb}(d_{HH})|_{allq}$ is much smaller than that of $V_{nb,ee}(d_{HH})$, $V_{nb,NN}(d_{HH})$, or $V_{nb,eN}(d_{HH})$ (vide infra).

Both electron−electron, $V_{nb,ee}(d_{HH})$, and nuclear−nuclear, $V_{nb,NN}(d_{HH})$, contributions to $V_{nb}(d_{HH})|_{allq}$ become increasingly negative with increasing d_{HH} in neopentane, whereas electron−nuclear terms, $V_{nb,eN}(d_{HH})$, become increasingly positive (Figures 11 and 12). Correlated values of $V_{nb,ee}(d_{HH})$, $V_{nb,NN}(d_{HH})$, and $V_{nb,eN}(d_{HH})$ were found to be slightly higher in magnitude than uncorrelated values. The largest contributions to $V_{nb}(d_{HH})|_{allq}$ are $V_{nb,ee}(d_{HH})$ and $V_{nb,eN}(d_{HH})$, which are opposite in sign and nearly equal in magnitude. In TMS, both the correlated and the uncorrelated values of $V_{nb,ee}(d_{HH})$, $V_{nb,NN}(d_{HH})$, and $V_{nb,eN}(d_{HH})$ vary with d_{HH} in a manner similar to that for neopentane except that, when d_{HH} values are scaled to account for the longer Si−C bond length, each of these energy terms is approximately half of the corresponding value in neopentane.

Plots of the relative contributions of $T_{nb}(d_{HH})$, $V_{nb,ee}(d_{HH})$, $V_{nb,NN}(d_{HH})$, and $V_{nb,eN}(d_{HH})$ to $V_{nb}(d_{HH})$ for neopentane and TMS are qualitatively similar at low and high d_{HH} values for both correlated and uncorrelated calculations. No single energy term is the dominant reason for the repulsive nature of $V_{nb}(d_{HH})|_{allq}$ in TMS at large d_{HH} (where $d_{HH} \geq \sum r_{vdW}$).

The individual energy contributions, $V_{nb,ee}(d_{HH})$, $V_{nb,NN}(d_{HH})$, $V_{nb,eN}(d_{HH})$, and $T_{nb}(d_{HH})$, were found to be functions of d_{HH}

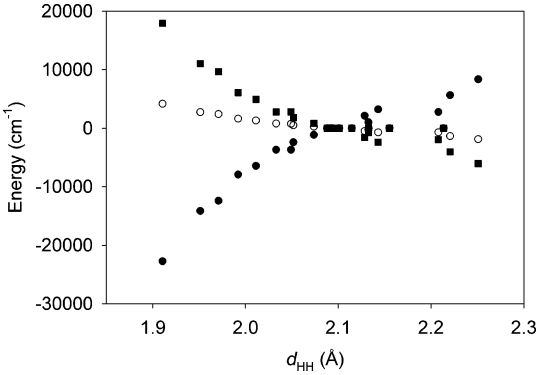

Figure 11. Contributions to the total site−site potential of electron−electron, $V_{nb,ee}(d_{HH})$ (squares), nuclear−nuclear, $V_{nb,NN}(d_{HH})$ (hollow circles), and electron−nuclear, $V_{nb,eN}(d_{HH})$ (solid circles), interactions for all q_L and q_C of the $\phi_L = \phi_C = 0°$ conformer of neopentane calculated at HF/6-311++G(2d,2p).

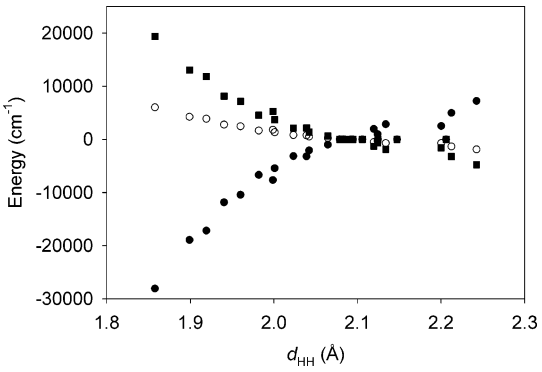

Figure 12. Contributions to the total site−site potential of electron−electron, $V_{nb,ee}(d_{HH})$ (squares), nuclear−nuclear, $V_{nb,NN}(d_{HH})$ (hollow circles), and electron−nuclear, $V_{nb,eN}(d_{HH})$ (solid circles), interactions for all q_L and q_C of the $\phi_L = \phi_C = 0°$ conformer of neopentane calculated at B3LYP/cc-pVTZ.

for the $\phi_L = \phi_C = 0°$ conformers of a *specific* molecule. Plots of $V_{nb,ee}(d_{HH})$, $V_{nb,NN}(d_{HH})$, $V_{nb,eN}(d_{HH})$, and $T_{nb}(d_{HH})$ as functions of d_{HH} for neopentane and TMS could not be superimposed upon one another because these contributions to $V_{nb}(d_{HH})|_{allq}$ are not transferable between TMS and neopentane.

The repulsive nature of $V_{nb}(d_{HH})|_{allq}$ in TMS at large d_{HH} was verified by an independent method, that is, CHelpG. In CHelpG, atomic and molecular charges are treated as fit parameters that are varied to reproduce the expectation value of the molecular electrostatic potential at the van der Waals surface.[28] Multipole-fit programs such as CHelpG suffer from electrostatic penetration effects at short ranges of interaction that result in an incomplete accounting of the electrostatic energy.[29] The CHelpG point charges presented in this paper are intended to give *qualitative* descriptions of charge interaction as a function of CH oscillator displacement. The surfaces of the van der Waals spheres on the hydrogen atoms in the $\phi_L = \phi_C = 0°$ conformer of neopentane interpenetrate one another for most displacements along q_L and q_C; therefore, only the CHelpG point charges for TMS will be presented.

CHelpG surfaces of the point charges on H_L and H_C as functions of displacements along both q_L and q_C for the $\phi_L = \phi_C = 0°$ and $\phi_L = \phi_C = 60°$ conformer of TMS were calculated at B3LYP/cc-pVDZ. The results for the $\phi_L = \phi_C = 0°$ conformer are presented in Figure 13. For both conformers, the point charges, $Q(e)$, on H_L and H_C are always of the same sign, indicating that the interaction between H_L and H_C is always repulsive over the range of q studied. The magnitude of the

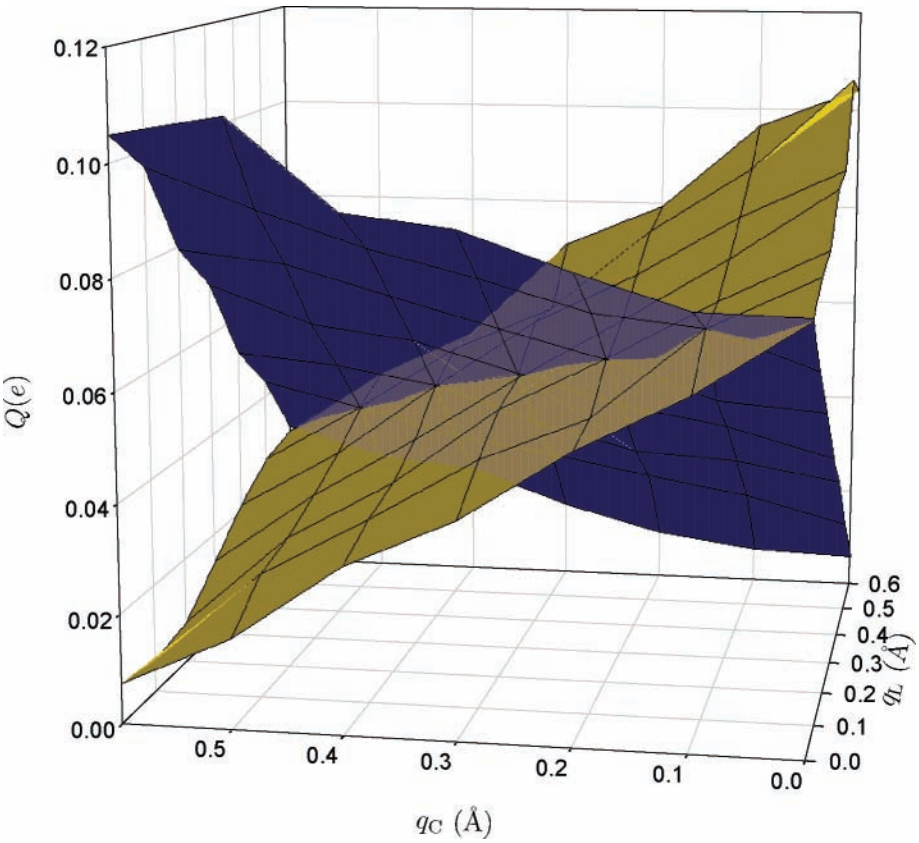

Figure 13. CHelpG point charges, $Q(e)$, fitted to the electrostatic potential for TMS ($\phi_L = \phi_C = 0°$ conformer) as functions of q_L and q_C for H atoms on CH oscillators CH_L (blue) and CH_C (yellow). Calculated at B3LYP/cc-pVDZ.

repulsive interactions are greater for the more crowded $\phi_L = \phi_C = 0°$ conformer where increases in q_L and q_C lead to a decrease in d_{HH}. The CHelpG calculations predict an electrostatic repulsion between H_L and H_C even at large d_{HH} in TMS.

The repulsive potential, $V_{nb}(d_{HH})|_{allq}$, does not rise sharply when $d_{HH} \ll \sum r_{vdW}$. van der Waals radii are relevant to through-space interactions where the interacting nuclei are not forced into close proximity by chemical bonds. In a case where covalently bound atoms are forced into close proximity, such as in neopentane and TMS, covalent radii[30] may provide a better lower limit on d_{HH} values beyond which $V_{nb}(d_{HH})|_{allq}$ rises sharply. The minimum value of d_{HH} observed in molecules is likely somewhere between r_{vdW} and r_{cov}.

There is no simple relationship between $V_{nb}(d_{HH})$ and the relative orientation of the H_L and H_C oscillators.

Local Mode Parameters. Local mode parameters $\tilde{\omega}$ and $\tilde{\omega}x$ were determined ab initio from fits of potential energy surfaces calculated at various conformations to a Morse potential (eq 1) for both neopentane and TMS. Data were calculated at HF/6-311++G(2d,2p) and B3LYP/cc-pVTZ and are presented in Tables 5 and 6, respectively. The ab initio determined values of $\tilde{\omega}$ and $\tilde{\omega}x$ at the $\phi_L = \phi_C = 60°$, $q_C = 0.00$ Å conformer were scaled relative to experimental values of $\tilde{\omega}$ and $\tilde{\omega}x$.[17,21] The range of q_L values was chosen to ensure wavefunction stability so that $q_L \in [-0.30, 0.50]$ Å for HF/6-311++G(2d,-2p) calculations and $q_L \in [-0.30, 0.70]$ Å for B3LYP/cc-pVTZ calculations. Step sizes were 0.10 Å for q_L.

Variables q_C, ϕ_L, and ϕ_C were varied independently. The ϕ values sampled were 0°, 30°, and 60°. The range of q_C values was subject to the same restrictions as q_L (vide supra) so as to maintain wavefunction stability. The maximum q_C displacement was 0.60 Å at B3LYP/cc-pVTZ and 0.50 Å at HF/6-311++G-(2d,2p).

TABLE 5: Scaled[a] ab Initio Local Mode Parameters for Neopentane and TMS Calculated at HF/6-311++G(2d,2p) for a Variety of Conformations

			parameters (cm^{-1}) from eq 1					
			neopentane		TMS		σ (cm^{-1}) from eq 2[b]	
ϕ_L (deg)	ϕ_C (deg)	q_C (Å)	$\tilde{\omega}$ (±2)	$\tilde{\omega}x$ (±0.3)	$\tilde{\omega}$ (±1)	$\tilde{\omega}x$ (±0.2)	neopentane	TMS
0	0	0.0	3072	60.8	3053	58.7	0.60	0.56
0	0	0.3	3084	57.5	3059	57.5	30	11
0	0	0.5	3093	55.4	3063	56.5	50	19
0	30	0.0	3065	60.7	3051	58.7	0.50	0.65
0	30	0.3	3074	58.3	3055	57.8	22	8.1
0	30	0.5	3081	56.7	3059	57.1	37	14
0	60	0.0	3058	60.7	3049	58.7	0.62	0.35
0	60	0.3	3063	59.5	3051	58.3	9.6	2.8
0	60	0.5	3067	58.8	3052	58.0	15	5.0
30	30	0.0	3066	60.6	3049	58.7	0.45	0.46
30	30	0.3	3076	57.9	3054	57.6	25	9.1
30	30	0.5	3084	56.2	3058	56.8	41	16
60	0	0.0	3048	60.5	3041	58.7	0.55	0.12
60	0	0.3	3052	59.3	3043	58.3	10	3.7
60	0	0.5	3056	58.4	3045	57.9	19	6.8
60	30	0.0	3054	60.5	3043	58.7	0.57	0.21
60	30	0.3	3061	58.8	3046	58.0	16	5.9
60	30	0.5	3066	57.5	3049	57.4	27	11
60	60	0.0	3049	60.5	3043	58.7	1.2	0.27
60	60	0.3	3055	59.2	3046	58.1	10	4.8
60	60	0.5	3059	58.3	3048	57.6	18	8.4

[a] Scaling factors employed for local mode parameters $\tilde{\omega}$ and $\tilde{\omega}x$ are given in ref 17. [b] σ denotes the estimated standard deviation of the fit of the unscaled ab initio calculated potential energy surface to eq 2.

It is expected that interaction between a vibrationally excited *X*H oscillator and some other part of the molecule will distort the *X*H vibrational potential away from the form given by eq 1.[1] Mohammadi and Henry[2] observed a decrease in $\tilde{\omega}x$ with

TABLE 6: Scaled[a] ab Initio Local Mode Parameters for Neopentane and TMS Calculated at B3LYP/cc-pVTZ for a Variety of Conformations

			parameters (cm^{-1}) from eq 1					
			neopentane		TMS		σ (cm^{-1}) from eq 2[b]	
ϕ_L (deg)	ϕ_C (deg)	q_C (Å)	$\tilde{\omega}$ (±2)	$\tilde{\omega}x$ (±0.3)	$\tilde{\omega}$ (±1)	$\tilde{\omega}x$ (±0.2)	neopentane	TMS
0	0	0.0	3069	60.9	3051	58.8	8.0	3.1
0	0	0.3	3072	59.4	3051	58.3	21	9.0
0	0	0.6	3073	58.3	3053	57.7	35	15
0	30	0.0	3063	60.9	3049	58.9	2.8	2.2
0	30	0.3	3068	59.5	3052	58.5	13	5.9
0	30	0.6	3073	58.3	3054	58.0	25	8.1
0	60	0.0	3058	60.8	3048	58.8	1.2	3.1
0	60	0.3	3062	60.0	3049	58.6	6.6	3.1
0	60	0.6	3065	59.3	3050	58.3	12	4.5
30	30	0.0	3062	60.8	3048	58.8	2.1	2.7
30	30	0.3	3066	59.4	3050	58.3	14	7.8
30	30	0.6	3068	58.4	3052	57.7	26	11
60	0	0.0	3050	60.7	3042	58.8	2.9	1.5
60	0	0.3	3052	60.0	3043	58.6	6.2	3.7
60	0	0.6	3055	59.2	3044	58.2	14	6.9
60	30	0.0	3053	60.6	3044	58.9	2.2	2.2
60	30	0.3	3056	59.7	3044	58.5	9.6	4.5
60	30	0.6	3059	58.7	3047	58.0	20	8.5
60	60	0.0	3049	60.5	3043	58.7	1.1	2.5
60	60	0.3	3052	59.8	3045	58.4	7.9	5.3
60	60	0.6	3055	59.0	3046	57.9	14	6.4

[a] Scaling factors employed for local mode parameters $\tilde{\omega}$ and $\tilde{\omega}x$ are given in ref 17. [b] σ denotes the estimated standard deviation of the fit of the unscaled ab initio calculated potential energy surface to eq 2.

increasing methyl substitution in butane, which is related to changes in the CH stretching potential. In neopentane, we observe an increase in $\tilde{\omega}$ and a decrease in $\tilde{\omega}x$ with increased steric hindrance in going from the $\phi_L = \phi_C = 60°$, $q_C = 0.00$ Å conformer to the $\phi_L = \phi_C = 0°$, $q_C = 0.60$ Å conformer at both HF/6-311++G(2d,2p) (Table 5) and B3LYP/cc-pVTZ (Table 6). There is a similar blue-shifting in the transition frequency in TMS; however, the magnitude of the increase in $\tilde{\omega}$ and decrease in $\tilde{\omega}x$ as ϕ_L, $\phi_C \rightarrow 0°$, $q_C \rightarrow 0.60$ Å is not as pronounced as that in neopentane where the steric crowding is higher.

The estimated uncertainties in $\tilde{\omega}$ and $\tilde{\omega}x$ are assumed to be identical to those in the experimental values[31] to which the ab initio parameters were scaled. At sterically hindered conformations, the scaled values of $\tilde{\omega}$ calculated at HF/6-311++G(2d,2p) (Table 5) are higher than those calculated at B3LYP/cc-pVTZ (Table 6). Similarly, scaled values of $\tilde{\omega}x$ calculated at HF/6-311++G(2d,2p) are lower than those calculated at B3LYP/cc-pVTZ. The blue-shifting of the local mode parameters becomes more pronounced with increased steric hindrance as ϕ_L, $\phi_C \rightarrow 0°$, and $q_C \rightarrow 0.60$ Å. The HF wavefunctions appear to be overestimating the energy of sterically hindered conformers. This overestimation is believed to be caused by the neglect of correlation, which should have an important influence at small separations, d_{HH} (vide supra).

Deviation from Morse Behavior. Ab initio PESs were fit to the Morse potential (eq 1) and to the generalized Morse potential (eq 2) in order to determine whether the Morse potential is a good basis in which to expand $V_{nb}(d_{HH})$. Particular attention has been paid to the effect of steric crowding on standard deviations. Displacements along q_L and q_C were restricted to the same range as done previously (vide supra) in order to ensure wavefunction stability.

The Morse potential in eq 1 has one scaling term and one expansion term, that is, D_e and a. The standard deviations in the fit of unscaled ab initio PESs to eq 1 for neopentane and TMS were found to be relatively constant and insensitive to molecular conformation. The mean estimated standard deviations of the fits at B3LYP/cc-pVTZ are 222 ± 16 cm^{-1} for all conformers of neopentane and 234 ± 6 cm^{-1} for all conformers of TMS. At HF/6-311++G(2d,2p), the mean estimated standard deviations of the fits are 151 ± 7 cm^{-1} for all conformers of neopentane and 147.1 ± 0.8 cm^{-1} for all conformers of TMS. Morse potentials of the form of eq 1 seem to be equally poor at describing unscaled ab initio PESs for both sterically hindered and unhindered conformers of neopentane and TMS.

We expect the quality of the fit will increase with an increasing number of expansion terms in the Morse potential. The generalized Morse potential (eq 2) has one scaling term and five expansion terms, that is, D_e, b_1, b_2, b_3, b_4, and b_5. The standard deviations, σ, of the fit of unscaled ab initio potential energy surfaces to the generalized Morse potential (eq 2) are given in Table 5 for neopentane and TMS at HF/6-311++G(2d,2p) and in Table 6 for neopentane and TMS at B3LYP/cc-pVTZ.

The values of σ are smaller for the generalized Morse potential eq 2 than for Morse potential eq 1 (vide supra) because (1) in general, the Morse potential is a good basis for describing an *X*H stretching potential, and (2) the inclusion of higher order terms serves to improve the fit. The suitability of the Morse potential as a basis in which to describe *X*H stretching potentials does not, however, imply that the Morse potential is a good basis in which to expand $V_{nb}(d_{HH})$ (vide infra).

In Tables 5 and 6 we note that the values of σ increase with increasing steric interaction. The Morse potential is a poor expansion basis for $V_{nb}(d_{HH})$ in neopentane and TMS because the site−site potentials in these molecules are approximately linear and not Morse- or Lennard−Jones-like (vide supra). Values of σ are higher for uncorrelated PESs than for correlated PESs for all but the least hindered conformers of neopentane and TMS. Correlation must be included for conformers where d_{HH} becomes small.

Conclusions

The nonbonded site−site potential between two proximal hydrogen atoms, H_L and H_C, located on different methyl groups was calculated at a given conformation, ϕ_L, ϕ_C, and q_C, by varying q_L. The resultant potential, denoted $V_{nb}(d_{HH})$, was expressed as a function of the separation between H_L and H_C, d_{HH}. The potential $V_{nb}(d_{HH})$ at a given q_C is pseudolinear for the $\phi_L = \phi_C = 0°$ conformers of neopentane and TMS at both HF/6-311++G(2d,2p) and B3LYP/cc-pVTZ. This potential was found to be conformation-dependent and was not transferable between molecules.

The plot of $V_{nb}(d_{HH})$ at all q_C for a $\phi_L = \phi_C = 0°$ conformer was denoted $V_{nb}(d_{HH})|_{allq}$. In neopentane and TMS this potential was found to be approximately linear in d_{HH}. This nonbonded site−site potential was neither Morse- nor Lennard−Jones-like. Lennard−Jones type models fail to predict the ab initio calculated $V_{nb}(d_{HH})$ at short intramolecular separations. The failure of simple, classical Lennard−Jones-type models to interpret nonbonded, site−site intramolecular energetics accurately raises concerns over the use of (classical) molecular mechanics force-fields to predict quantum effects such as $V_{nb}(d_{HH})$ in sterically hindered molecules.

The individual kinetic, electron−electron, electron−nucleus, and nucleus−nucleus contributions to $V_{nb}(d_{HH})|_{allq}$ were calculated at HF/6-311++G(2d,2p) and B3LYP/cc-pVTZ for the $\phi_L = \phi_C = 0°$ conformers of neopentane and TMS. The largest

individual contributions at small d_{HH} are electron−electron repulsion and electron−nucleus attraction.

The potential $V_{nb}(d_{HH})|_{allq}$ was found to be repulsive at all d_{HH} in both neopentane and TMS at HF/6-311++G(2d,2p) and B3LYP/cc-pVTZ. This is surprising because one would expect, on the bases of van der Waals radii and Lennard−Jones potentials, that the nonbonded site−site potential between H_L and H_C would become attractive when $d_{HH} > \sum r_{vdW}$. The repulsive nature of $V_{nb}(d_{HH})|_{allq}$, even where $d_{HH} > \sum r_{vdW}$, was verified by CHelpG calculations in TMS. The explicit inclusion of electron correlation at the MP2/6-31G(d,p) level of theory and basis set size gave similar results.

The repulsive potential, $V_{nb}(d_{HH})|_{allq}$, did not rise sharply when $d_{HH} \ll \sum r_{vdW}$. The reason for this may be that a network of covalent bonds force nonbonded atoms into separations less than the sum of their van der Waals radii. Covalent radii may provide a better lower limit for d_{HH} values beyond which $V_{nb}(d_{HH})|_{allq}$ rises sharply.

Local mode parameters $\tilde{\omega}$ and $\tilde{\omega}x$ were calculated ab initio for neopentane and TMS at various degrees of steric hindrance by varying ϕ_L, ϕ_C, and q_C. As $\phi_L, \phi_C \rightarrow 0°$ and $q_C \rightarrow q_{C,max}$ (where $q_{C,max}$ is the maximum displacement value along q_C), steric hindrance approached a maximum and we observed that the magnitude of $\tilde{\omega}$ increased and the magnitude of $\tilde{\omega}x$ decreased because of the additional (steric) barrier to high amplitude vibration. The increase in $\tilde{\omega}$ and decrease in $\tilde{\omega}x$, which led to a blue-shift in transition frequencies, were more pronounced in neopentane than in TMS because of the higher degree of steric hindrance in the former.

The effect of the inclusion of electron correlation is to (1) decrease the repulsive through-space site−site potential at small d_{HH} and (2) lessen both the increase in ab initio calculated $\tilde{\omega}$ values and the decrease in ab initio calculated $\tilde{\omega}x$ values at sterically hindered conformers. In both cases, electron correlation substantially lessens the energy of conformers where d_{HH} is small.

Acknowledgment. Funding for this research has been provided by the Natural Sciences and Engineering Council of Canada.

References and Notes

(1) Petryk, M. W. P.; Henry, B. R. *J. Phys. Chem. A* **2002**, *106*, 8599.
(2) Mohammadi, M. A.; Henry, B. R. *Proc. Natl. Acad. Sci. U.S.A.* **1981**, *78*, 686.
(3) Moss, D. B.; Parmenter, C. S.; Ewing, G. E. *J. Chem. Phys.* **1987**, *86*, 51.
(4) Martens, C. C.; Reinhardt, W. P. *J. Chem. Phys.* **1990**, *93*, 5621.
(5) Mannfors, B.; Sundius, T.; Palmö, K.; Pietilä, L.-O.; Krimm, S. *J. Mol. Struct.* **2000**, *521*, 49.
(6) Palmö, K.; Mirkin, N. G.; Krimm, S. *J. Phys. Chem. A* **1998**, *102*, 6448.
(7) Morse, P. M. *Phys. Rev.* **1929**, *24*, 57.
(8) Sage, M. L.; Jortner, J. *Adv. Chem. Phys.* **1981**, *47*, 293.
(9) Wright, J. S.; Williams, R. J. *J. Chem. Phys.* **1983**, *79*, 2893.
(10) Henry, B. R. The Local Mode Model. In *Vibrational Spectra and Structure*; Durig, J. R., Ed.; Elsevier Scientific: Amsterdam, 1981; Vol. 10.
(11) Watson, I. A.; Henry, B. R.; Ross, I. G. *Spectrochim. Acta, Part A* **1981**, *37*, 857.
(12) Mortensen, O. S.; Henry, B. R.; Mohammadi, M. A. *J. Chem. Phys.* **1981**, *75*, 4800.
(13) Kjaergaard, H. G.; Yu, H.; Schattka, B. J.; Henry, B. R.; Tarr, A. W. *J. Chem. Phys.* **1990**, *93*, 6239.
(14) Sowa, M. G.; Henry, B. R.; Mizugai, Y. *J. Phys. Chem.* **1991**, *95*, 7659.
(15) Low, G. R. Calculation of OH-Stretching Vibrational Properties of Water Clusters. Thesis, University of Otago, 2001.
(16) Low, G. R.; Kjaergaard, H. G. *J. Chem. Phys.* **1999**, *110*, 9104.
(17) Petryk, M. W. P.; Henry, B. R. *J. Phys. Chem. A* **2005**, *109*, 4081.
(18) Frisch, M. J.; Trucks, G. W.; Schlegel, H. B.; Scuseria, G. E.; Robb, M. A.; Cheeseman, J. R.; Zakrzewski, V. G.; Montgomery, J. A., Jr.; Stratmann, R. E.; Burant, J. C.; Dapprich, S.; Millam, J. M.; Daniels, A. D.; Kudin, K. N.; Strain, M. C.; Farkas, O.; Tomasi, J.; Barone, V.; Cossi, M.; Cammi, R.; Mennucci, B.; Pomelli, C.; Adamo, C.; Clifford, S.; Ochterski, J.; Petersson, G. A.; Ayala, P. Y.; Cui, Q.; Morokuma, K.; Malick, D. K.; Rabuck, A. D.; Raghavachari, K.; Foresman, J. B.; Cioslowski, J.; Ortiz, J. V.; Stefanov, B. B.; Liu, G.; Liashenko, A.; Piskorz, P.; Komaromi, I.; Gomperts, R.; Martin, R. L.; Fox, D. J.; Keith, T.; Al-Laham, M. A.; Peng, C. Y.; Nanayakkara, A.; Gonzalez, C.; Challacombe, M.; Gill, P. M. W.; Johnson, B. G.; Chen, W.; Wong, M. W.; Andres, J. L.; Head-Gordon, M.; Replogle, E. S.; Pople, J. A. *Gaussian 98*, revision A.5; Gaussian, Inc.: Pittsburgh, PA, 1998.
(19) Frisch, M. J.; Trucks, G. W.; Schlegel, H. B.; Scuseria, G. E.; Robb, M. A.; Cheeseman, J. R.; Zakrzewski, V. G.; Montgomery, J. A., Jr.; Stratmann, R. E.; Burant, J. C.; Dapprich, S.; Millam, J. M.; Daniels, A. D.; Kudin, K. N.; Strain, M. C.; Farkas, O.; Tomasi, J.; Barone, V.; Cossi, M.; Cammi, R.; Mennucci, B.; Pomelli, C.; Adamo, C.; Clifford, S.; Ochterski, J.; Petersson, G. A.; Ayala, P. Y.; Cui, Q.; Morokuma, K.; Malick, D. K.; Rabuck, A. D.; Raghavachari, K.; Foresman, J. B.; Cioslowski, J.; Ortiz, J. V.; Stefanov, B. B.; Liu, G.; Liashenko, A.; Piskorz, P.; Komaromi, I.; Gomperts, R.; Martin, R. L.; Fox, D. J.; Keith, T.; Al-Laham, M. A.; Peng, C. Y.; Nanayakkara, A.; Gonzalez, C.; Challacombe, M.; Gill, P. M. W.; Johnson, B. G.; Chen, W.; Wong, M. W.; Andres, J. L.; Head-Gordon, M.; Replogle, E. S.; Pople, J. A. *Gaussian 98*, revision A.11; Gaussian, Inc.: Pittsburgh, PA, 2001.
(20) Frisch, M. J.; Trucks, G. W.; Schlegel, H. B.; Scuseria, G. E.; Robb, M. A.; Cheeseman, J. R.; Montgomery, J. A., Jr.; Vreven, T.; Kudin, K. N.; Burant, J. C.; Millam, J. M.; Iyengar, S. S.; Tomasi, J.; Barone, V.; Mennucci, B.; Cossi, M.; Scalmani, G.; Rega, N.; Petersson, G. A.; Nakatsuji, H.; Hada, M.; Ehara, M.; Toyota, K.; Fukuda, R.; Hasegawa, J.; Ishida, M.; Nakajima, T.; Honda, Y.; Kitao, O.; Nakai, H.; Klene, M.; Li, X.; Knox, J. E.; Hratchian, H. P.; Cross, J. B.; Bakken, V.; Adamo, C.; Jaramillo, J.; Gomperts, R.; Stratmann, R. E.; Yazyev, O.; Austin, A. J.; Cammi, R.; Pomelli, C.; Ochterski, J. W.; Ayala, P. Y.; Morokuma, K.; Voth, G. A.; Salvador, P.; Dannenberg, J. J.; Zakrzewski, V. G.; Dapprich, S.; Daniels, A. D.; Strain, M. C.; Farkas, O.; Malick, D. K.; Rabuck, A. D.; Raghavachari, K.; Foresman, J. B.; Ortiz, J. V.; Cui, Q.; Baboul, A. G.; Clifford, S.; Cioslowski, J.; Stefanov, B. B.; Liu, G.; Liashenko, A.; Piskorz, P.; Komaromi, I.; Martin, R. L.; Fox, D. J.; Keith, T.; Al-Laham, M. A.; Peng, C. Y.; Nanayakkara, A.; Challacombe, M.; Gill, P. M. W.; Johnson, B.; Chen, W.; Wong, M. W.; Gonzalez, C.; Pople, J. A. *Gaussian 03*, revision B.03; Gaussian, Inc.: Wallingford, CT, 2003.
(21) Petryk, M. W. P. Local Mode Vibrational Overtones of Sterically Crowded Molecules. Thesis, University of Guelph, 2004.
(22) Pauling, L. *The Nature of the Chemical Bond*, 3rd ed.; Cornell University Press: Ithaca, NY, 1960.
(23) Sibert, E. L., III; Hynes, J. T.; Reinhardt, W. P. *J. Chem. Phys.* **1984**, *81*, 1135.
(24) Wildman, T. A. *Chem. Phys. Lett.* **1980**, *75*, 383.
(25) Wiberg, K. B.; Rablen, P. R. *J. Comput. Chem.* **1993**, *14*, 1504.
(26) Mannfors, B.; Palmö, K.; Krimm, S. *J. Mol. Struct.* **2000**, *556*, 1.
(27) Breneman, C. M.; Wiberg, K. B. *J. Comput. Chem.* **1990**, *11*, 361.
(28) Szefczyk, B.; Sokalski, W. A.; Leszczynski, J. *J. Chem. Phys.* **2002**, *117*, 6952.
(29) White, J. C.; Davidson, E. R. *J. Mol. Struct.: THEOCHEM* **1993**, *282*, 19.
(30) Wells, A. F. *Structural Inorganic Chemistry*; Clarendon Press: Oxford, 1962.
(31) Petryk, M. W. P.; Henry, B. R. *Can. J. Chem.* **2001**, *79*, 279.